A general evolutionary model for the emergence of novel characters from serial homologs

Daohan Jiang[1], Matt Pennell[2], Lauren Sallan[1*]

[1]Macroevolution Unit, Okinawa Institute of Science and Technology Graduate University, Onna-son, Okinawa 904-0497 Japan.

[2]Department of Computational Biology, Cornell University, Ithaca, NY 14853, USA.

*Corresponding author. Email: lauren.sallan@oist.jp

The origin of morphological characters with novel forms and functions is among the most fascinating phenomena in evolution, and understanding its underlying principles has been a fundamental goal of evolutionary biology. An essential means by which novelties evolve is the divergence of repeated body parts, known as serial homologs, into various forms, as in the case of tetrapod limbs and insect wings. However, the mechanisms underlying such processes are poorly understood, with systematic investigations hindered by the lack of a generalized model that links selective, genetic, and developmental mechanisms and the expected patterns of evolutionary dynamics. To fill this gap, we propose a generalizable model for the evolution of serial homologs that is founded on recent advances in developmental biology, where the development of each serial homolog is controlled via a hierarchical gene regulatory network consisting of genes that specify character identity and those that encode the specific phenotypic state. Under this model, we investigated two types of evolutionary novelties: divergence in character states between body parts with conserved identities and switching of character identity by turning on and off master regulators. Using population

genetic simulations with different regimes of selection and developmental constraints, we demonstrate how selection and developmental constraints interact to shape dynamics of phenotypic evolution and conditions under which each type of novelty is likely to evolve. Together, our results provide general insights into how novelties could evolve from serial homologs, and offer a modeling framework where the developmental evolution of a broad range of phenotypic characters can be studied.

Introduction

To understand mechanisms underlying the origin of novel characters has been a fundamental goal of evolutionary biology. An essential means by which novelties emerge is the divergence of repeated ancestral characters known as serial homologs (*1–3*). A plethora of such novelties have been documented. Notable examples of serial homologs that develop into distinct forms include paired fins and limbs of vertebrates, tetrapods' digits, vertebrae, gill arches, skin appendages (e.g., scales, feathers, hair), body segments of arthropods and paired appendages attached to them, components of angiosperm flowers, and cell types (*3*). Central to the problem of evolutionary novelties is how developmental processes can constrain and bias the trajectory of of evolution. It has been proposed that developmental constraints, in general, can have a dispositional effect on phenotypic evolution by channeling the effect of mutations on the phenotype and thereby biasing the availability of genetic variations (*4–12*). Developmental constraints are particularly relevant to phenotypic divergence between serial homologs: in contrast to homologous characters of different species (e.g., forelimbs of different tetrapod species), which can undergo phenotypic divergence as different lineages acquire different genomic substitutions, serially homologous body parts of the same organism (e.g., forelimbs and hindlimbs of the same animal) are encoded by the same genome. For serial homologs to become novelties, otherwise identical developmental processes that take place repeatedly in the same organism must become different. The divergence of serial homologs, therefore, needs to be understood in the light of development.

Advancements in developmental biology over the past few decades have shed light on molecular mechanisms underlying the development of serial homologs and how they could have evolved into

novel forms. Phenotypic similarity between serial homologs results from similar gene expression programs during their development—i.e., which genes are expressed, their expression levels, and timing of their expression; by the same principle, difference in the gene expression programs is responsible for phenotypic variation among the otherwise identical serial homologs (*3, 13–16*). Observed differences in expression have, in many cases, been hypothesized or confirmed as attributable to master regulator genes that activate or suppress many other genes and/or pathways. Expression of such genes specify the identity of a body part, but not necessarily specific character states (the observable realized phenotype). That is, the expression profile of these genes are shared by of homologous body parts of different species, regardless of how different their forms are (*3, 14, 15*). A well documented case of such regulator is the *Ultrabithorax* (*Ubx*) gene, whose expression specifies identity of hindwings in insects. Loss of *Ubx* expression causes forewings to grow at the position of hindwings, regardless of specific size or morphology of the wings: in fruit flies, the perturbation causes the halteres to be replaced by 'normal' wings, whereas in beetles, it is hindwings being replaced by elytra (*17–24*). Another example where pathways underlying character identities have been well-studied is that of tetrapod limbs, in which case two *T-box* genes, *Tbx4* and *Tbx5*, specify forelimb and hindlimb identities respectively but not specific limb morphologies (*25–31*). In addition to morphological characters, identities of cell types are also found to be regulated in similar ways (e.g., (*32–35*)).

Despite the progress in understanding the underlying developmental mechanisms, their evolutionary implications have not yet been systematically investigated. While quantitative predictions are rare, there have indeed been models that make qualitative predictions about how evolution would be constrained by developmental processes. A prime example of such predictions is that concerning genetic mechanisms of morphological evolution: because homeobox (*Hox*) genes regulating development are highly pleiotropic, mutations that alter the sequence of proteins they encode are likely strongly deleterious; as a result, it is substitutions in their *cis*-regulatory elements (i.e., DNA segments linked to a gene and regulating its expression via interacting with DNA-binding proteins) that are more likely to contribute to morphological evolution (*36*). There have also been developmental models that make predictions about specific character states that can potentially occur during evolution. A model would be supported if a predicted intermediate form did exist in the fossil record or matched modern developmental stages (recapitulation), and rejected if forms predicted to be

implausible are observed. For instance, the model for feather development proposed by Prum (*37*) makes predictions about possible forms of early feathers, which are supported by findings in various early-diverging coelurosaur groups (*38*). Another example of developmental models (un)supported by fossil evidence is how a growth series of the non-teleost ray-finned fish *Aetheretmon valentiacum* overturns a classic model of recapitulation of evolutionary stages during teleost tail development while supporting an alternative model of derived states for non-homologous structures (*39*). Developmental models that make quantitative predictions about evolution dynamics, in contrast, are rare to our knowledge. Examples of such models include those for mollusk shells (*40, 41*) and for mammalian molars (*42*), the latter of which allowed developmental constraints to be incorporated in phylogenetic comparative analyses to study the evolutionary dynamics (*43*). To date, there has not yet been a generalized model under which one can investigate and analyze quantitatively how features of developmental processes shape phenotypic evolution. Furthermore, present models mainly emphasize how development limits the course of evolution, whereas the interplay between developmental constraints and adaptation, which is presumably essential in the origin of novel characters, is less well understood.

To fill these gaps, we present a mathematical model that incorporates key general features of gene regulatory networks underlying the development of serially homologous characters, and explore its implications for phenotypic evolution and novelties. Under this model, the character state of a body part is controlled via a hierarchical gene regulatory network consisting of two classes of genes: the identity determination genes (IDGs) and the state determination genes (SDGs). The IDGs are master regulators that regulate the expression of SDGs, and the SDGs are effector genes that produce the phenotype. IDGs are named so because their expression specifies character identity (e.g., if a tetrapod limb is a forelimb or a hindlimb), and SDGs are named so as they control the character state (e.g., size and shape of a limb). Biologically, an IDG in our model can either be interpreted as a single gene encoding a *trans*-regulatory factor (e.g., aforementioned examples of *Ubx*, *Tbx4*, and *Tbx5*), or a set of co-expressed genes that act together to specify the character identity, also known as a character identity network (*3, 15, 44, 45*) or a core regulatory complex underlying a cell type identity (*46*). Similarly, an SDG can also be interpreted as a set genes that are co-regulated by the same IDGs.

Under this modeling framework, we investigated two types of evolutionary novelties. The first

type of novelty we examined is the divergence in character states between serial homologs with conserved identities. These characters have distinct IDG expression programs that are conserved during evolution, and divergence in character states due to substitutions *cis*-regulatory elements that interact with the IDGs to regulate SDG expression. When IDGs expressed in two serial homologs have different targets with different phenotypic effects, or if their shared targets respond differently to them, different character states can be produced (Fig. 1A). Prime examples of such characters include the aforementioned cases of tetrapod limbs and insect wings, among others. The other type of novelty we examined is the turnover of character identity mediated by change in the expression of IDG(s). As each IDG can regulate the expression of many SDGs, alteration of the expression of one or a few IDGs can also alter expression states of many SDGs, potentially leading to drastic phenotypic changes (Fig. 1B). A putative example of this type of evolutionary change is the transition between feathers and scales states in birds as well as non-avian theropods: mechanistically, such a conversion can be achieved by simply activating or suppressing *Sonic Hedgehog* (*Shh*) signaling (in given body regions) (*47–49*); on the other hand, there is indeed substantial diversity in the spatial distribution of feathers among theropods (*38, 50*), which could have been mediated by genetic changes that altered the expression of master regulators like *Shh*. To explore principles underlying these two types of evolutionary novelties, we performed individual-based population genetic simulations using SLiM (*51*). By examining evolutionary dynamics in a variety of evolutionary scenarios, we explored conditions under which each type of novelty is likely to evolve, demonstrating how patterns of evolution are connected to the underlying mechanisms.

Results

An generalizable developmental model for serially homologous characters

In our model, we assume that there are n IDGs and m SDGs that can potentially be expressed in each serial homolog. Expression levels of the IDGs in a given serial homolog are determined collectively by a local *trans*-regulatory environment and the IDGs' *cis*-regulatory element(s). The relationship can be represented mathematically as $\mathbf{X} = \mathbf{C} \circ \mathbf{L}$, where $\mathbf{X}$ is a vector of length n containing expression levels of all IDGs and an element-wise product of $\mathbf{C}$ and $\mathbf{L}$. Each element of

L captures the effect of an IDG's *cis*-regulatory element(s) on its baseline expression. Each element of **C** recapitulates the effect of the local *trans*-regulatory environment, which is specific to the serial homolog under consideration, on the expression of a given IDG; when an element of **C** is equal to zero, the corresponding IDG is not expressed. More specifically, **C** reflects the effect of early stage processes that give rise to the distinct fates of different cell populations before phenotypes of interest are formed, such as positional signal from a morphogen gradient (*52*). Expression levels of SDGs are then given by $\mathbf{Y} = \exp(\mathbf{AX})$, where **Y** is a vector of length m and **A** is an $m \times n$ matrix. The **A** matrix characterizes IDGs' per-unit-expression regulatory effect on SDGs' expression—e.g., element $A_{i,j}$ of **A** represents the effect of the j-th IDG on expression of the i-th SDG. Elements of **A** capture strength and direction of interactions between *cis*-regulatory sequences of the SDGs and the IDGs: a positive value represents an activation effect, whereas a negative value represents repression. At last, the realized character state, represented by a d-dimensional vector, is given by $\mathbf{z} = \mathbf{B} \ln \mathbf{Y}$, where **B** is a $d \times n$ matrix characterizing the per-unit-expression-level effect of SDGs on the phenotype (see also Materials and Methods).

In this study, we considered two types of genetic changes affecting developmental regulation, which correspond to two types of evolutionary novelties we focused on. The first is change in elements of **A**, mediated by mutations in *cis*-elements that interact with IDGs to regulate the expression of SDGs; such genetic changes can alter the character state and cause character state divergence between serial homologs with distinct identities (Fig. 1A). The second type of genetic change affect elements of **C**; by altering the local *trans*-regulatory environment, IDG expression in a particular body part and thus the said body part's identity can be altered (Fig. 1B). As demonstrated below, the two types of genetic changes can potentially give rise to evolutionary novelties given appropriate regimes of selection.

Character state divergence of serial homologs with conserved identities

We simulated the coevolution of two serially homologous characters with distinct identities, each specified by a respective IDG. Elements of **C** and **L** are constant such that IDG expression is conserved over time in both serial homologs; evolutionary changes in character state are mediated by mutations in *cis*-elements of SDGs. We considered scenarios where the two IDGs share different

proportions of target SDGs. When an SDG is a shared target of two IDGs, mutations in its *cis*-regulatory elements will tend to have concordant effects on its response to two IDGs, and consequently concordant effects on its expression in two serial homologs.

We considered three scenarios of directional selection (Fig. 2A). In the first scenario, only one serial homolog's character state (z_1) is under directional selection for a greater value while the other serial homolog's (z_2) is under stabilizing selection. The second scenario is referred to as a scenario of diversifying selection, as the optimum value of z_1 is greater than the ancestral state and whereas the optimal z_2 is smaller than the ancestral state. In the last scenario, which is referred to as a scenario of concordant selection, greater values of both z_1 and z_2 are selected for. In the absence of any genetic constraint, phenotypic divergence between serial homologs is expected to increase in the first two scenarios, but not the third one. In addition, we considered three regimes of correlational selection: a scenario where correlational selection is absent, a scenario of positive correlational selection where the optimal scaling line has a positive slope (Fig. 2A, orange lines), and a scenario of negative correlational selection where the optimal scaling line has a negative slope (Fig. 2A, purple lines). Together, nine combinations of directional and correlational selection were examined (see also Materials and Methods). In scenarios with no correlational selection, the adaptive landscape is characterized by a single fitness peak. When correlational selection is present, the adaptive landscape is characterized by a fitness ridge (specified by the optimal scaling line) and a peak along this ridge. As a negative control, we also simulated evolution under stabilizing selection in combination with three regimes of correlational selection. We performed simulations in both Wright-Fisher (WF) populations, which have a constant size, and non-WF populations, whose size can change over time as a result of unequal numbers of birth and death. In WF populations, adaptive evolution, while causing the population's mean phenotype to change, is inconsequential to the population's growth or survival. In the non non-WF populations, we implemented a setting of density-dependence, where the death rate of each individual increases with the population size. An individual's death rate is also affected by its phenotype, increasing with distance from the optimum. Together, a population consisting of individuals with more optimized phenotypes will have minimized overall death rate (given population size), and can maintain an equilibrium population size equal to the carrying capacity.

In WF populations, as expected, phenotypic divergence between serial homologs generally

increased when only one serial homolog is subject to selection (Fig. 2B-D) or when two serial homologs are under divergent selection (Fig. 2E-G). In both scenarios, the magnitude of divergence decreases with the fraction of targets shared between two IDGs (Fig. 2B-G), demonstrating the impact of developmental constraint on evolution. In contrast, in the face of concordant selection, two serial homologs had similar character states, regardless of the number of targets shared between SDGs (Fig. 2H-J). Evolutionary change of z_1, which had the same optimum in all scenarios, showed similar trends (Fig. S1). In two scenarios where correlational selection is present and the ancestral state is not along the line of optimal scaling, there is less divergence between serial homologs (Fig. 2F, I) and less adaptive evolutionary change in z_1 (Fig. S1F, I), reflecting the fact that the populations started from a state where fitness is low and increases slowly with phenotype. Populations subject to stabilizing selection, as expected, showed little character state divergence between serial homologs (Fig. S2A-C); the number of targets shared by the IDGs, did have an impact on variance of divergence (Fig. S2D-F) as well as correlation between serial homologs across populations (Fig. S2G-I).

In non-WF populations, sharing of targets between IDGs similarly resulted in constraints on adaptive phenotypic evolution when two serial homologs had different optima but not in the scenario of concordant selection (Fig. S3-S4). Population sizes at the end of the simulation show consistent trends (Fig. S5), indicating adaptive response at the phenotypic level indeed translates into consequence for population growth. Under the two conditions where the ancestral state is off the adaptive ridge, the populations underwent little adaptive phenotypic evolution (Fig. S3E, I; Fig. S4E, I) and had small population sizes (Fig. S5E, I). Together, results from WF and non-WF populations show consistent trends regarding the impact of developmental constraints and regime of selection on character state divergence.

Turnover of character identities

To investigate conditions under which character identity shifts could happen, we considered a character that can assume one of two potential identities (denoted I_1 and I_2, of which I_1 is ancestral) by expressing two different IDGs with distinct targets; as SDGs regulated by two IDGs affect the phenotype differently, two identities correspond to two distinct character states. Which IDG to

express in a given body part is determined by the local concentration of a morphogen, c. When c is equal to or beyond a cutoff, character identity will be I_1; otherwise, it will be I_2. The ancestral value of c is equal to the cutoff, so the ancestral character identity is I_1, and a mutation that lowers c will alter the identity. We performed simulations under five regimes of selection characterized by different optimal phenotypes. Given that all other regulatory parameters are equal to the ancestral values, the 5 optima are respectively 1) the phenotype produced by the non-ancestral identity, I_2, 2) an intermediate phenotype between those produced by I_1 and I_2 but close to the latter the phenotype produced by I_2, 3) an intermediate phenotype right in between those produced by I_1 and I_2, 4) an intermediate phenotype that is closer to that produced by I_1, and 5) the phenotype produced by I_1. In scenarios 1) and 2), a half of mutation that affects c are adaptive (i.e., bringing the phenotype closer to the optimum) on an ancestral genetic background and the rest are neutral; in scenario 3), such mutations are all neutral, as phenotypes produced by two identities are equally distant from the optimum; in scenario 4) and 5), a half mutations neutral on an ancestral genetic background and the rest are deleterious (Fig. 3A). Given the distribution of mutations' fitness effects, we predict that character identity is more likely to be shift to I_2 in 1) and 2), less likely in 3), and most unlikely in 4) and 5).

As predicted, I_2 evolved in most of the simulated population in 1), where the optimum is the character state it produces (Fig. 3B); even in populations where I_2 is not fixed, it has high frequency, resulting in a high *trans*-genotypic value for the corresponding IDG's expression (Fig. 3C). Very similar patterns were observed in 2), where the optimum is not the same but still close to the character state produced by I_2 (Fig. 3B-C), indicating an identity shift can happen even if a shift does not lead to the exact optimal phenotype. Identity shift happened relatively infrequently in 3) and did not happen in 4) and 5) when the optimum is closer to the phenotype produced by the ancestral identity I_1 (Fig. 3B-C).

We also performed simulations in non-WF populations. Trends were consistent with those seen in WF populations but stronger: I_2 was fixed when the optimum is at or close to the character state I_2 produces (scenarios 2) and 5)), and had zero frequency under other conditions (Fig. S6A-B). We also found that larger population sizes were reached in 1) and 2) than in 3), despite the optimum is closer to the ancestral state in 3), as identity shift provides a quick pathway for adaptation in 1) and 2) but not 3). Together, our results show that identity shift can facilitate adaptation when the new

optimum is in the vicinity of a character state that can potentially be produced by an alternative character identity.

Discussion

In this study, we present a generalizable model for the development of serially homologous characters that incorporate features of the underlying gene regulatory networks. Under the general modeling framework, we examined on two scenarios of evolution, the first being character state divergence between characters with conserved identities mediated by evolutionary changes in regulatory elements that interact with IDGs to regulate SGD expression. For these characters, we observed character state divergence when two serial homologs had different homologs; under these regimes of selection, we also found the rate of divergence in character states to be faster when IDGs underlying different identities share a smaller portion of targets (Fig. 2, Fig. S3), which is consistent with the notion that decoupling of developmental regulation of different serial homologs enhances evolvability and allows more diverse combinations to evolve (*53*). Our model for such characters can potentially help us understand a broad range of novel character states. A potential example of character state innovation via regulatory evolution is how bats evolved long forelimbs: substitutions in an enhancer increased the expression level of *Prx1*, a gene that does not specify limb identities, in developing forelimb bones, resulting in forelimb elongation (*54*). Similarly, limb size reduction, which has taken place repeatedly in various tetrapod lineages, could also be mediated by similar evolutionary mechanisms (note that the complete loss of limbs is more appropriately a loss of character identity (*55*) rather than an extreme character state, albeit potentially driven by similar selection regimes). The other type of novelty we examined is switching of character identity via turning on and off IDGs. We found such evolutionary changes are likely to occur when the optimum is closer to the phenotype produced by the derived identity than that produced by the ancestral identity (Fig. 3, Fig. S6) and can potentially happen even when identity switching is neutral (Fig. 3). Scenarios examined in our simulations can potentially explain drastic evolutionary changes between apparently discrete states arising from the same developmental cell lines in similar positions, such as the conversion between feathered and scaled states in dinosaurs.

For known cases of evolutionary novelties, it is often unclear if the observed states resulted

from character identity changes, character state changes, or acquired through loss and replacement rather than fully homologous; more developmental studies will be necessary to determine how broad a range of novelties are explained by either of the two types of scenarios examined in this study. A general approach to distinguishing evolutionary changes of character identity and state is to compare the effect of the same genetic or gene expression perturbation across species. Specifically, one can test if the same perturbation produce similar character states in different species, or affect homologous characters of different species while producing dissimilar character states. A prime example of such investigations is the aforementioned case of *Ubx*. In both fruit flies and beetles, hindwings are replaced by forewings upon loss of *Ubx* expression while the resulting character state changes differ in the two groups, indicating the gene is responsible for specifying hindwing identity but not specific character states of halteres or 'normal' wings (*15, 17–24*). Hence, evolutionary changes mediated by *Ubx* expression evolution shall be interpreted as identity instead of state changes. More such investigations will be necessary to clarify the nature of other instances of novelties and understand the underlying evolutionary mechanisms using our model.

In each of our simulations, for simplicity, we considered only two distinct character identities. If the coevolution of three or more serial homologs is being investigated, in contrast, the relationship between them will become relevant, as not all character identities originated at the same time, and are historically related to each other in a way that can be characterized with a phylogenetic tree (*3, 16, 33, 35, 56*). The structure of such a character tree can have key implications for coevolutionary dynamics of serial homologs. Importantly, as IDG expression programs that diverged from each other more recently likely share more genes and targets than those that diverged earlier, patterns of character state divergence between serial homologs will reflect a combined effect of selection on individual characters and the phylogenetic relationship among them, which need to be teased apart with appropriate correction methods. In addition, there exist novel identities that appear to have originated by 'hybridizing' pre-existing expression programs, as in the case of novel secretary cell types in rove beetles (*57, 58*); coevolutionary dynamics of such characters and others is an open question that shall be explored in future studies.

We examined models of selection where the relationship between phenotype and fitness is specified while mechanisms underlying the relationship are not. However, such simple models can also represent more specific scenarios of potential interest. For example, negative correlational

selection could be mediated by selection for division of labor in response to trade-off between functions performed by the same body part (*59*). Apparent negative correlation selection can also be a result of selection on a composite trait—e.g., selection for an optimal total length of two regions of the vertebral columns could make lengths of the two regions negatively scaled along the line of optimal combinations. Our modeling framework can readily be developed to explore implications of specific mechanisms of selection; one can introduce variables that mediate the effect of the phenotype on fitness—e.g., locomotion and foraging performance and model them as custom-define functions of the character state.

Models of adaptation examined in this study are simple models concerning a single episode of adaptive evolution toward a pre-specified optimum. Another class of models that would be of interest is models with moving adaptive landscapes, which may better explain variation in the distribution of phenotypes across divergent clades. In addition, movement of the adaptive landscape can potentially interact with developmental constraints to shape patterns macroevolutionary divergence—e.g., when there is strong developmental (and thereby genetic) constraint, populations track the moving optimum less well and may end up stranded near an ancestral state and display less evolutionary divergence (*60*). It remains an open question, however, whether adaptive landscapes' movement is generally predictable, and if so, how they move (*61, 62*). For body parts with positional identities, there could also be correlation between their identity and functional constraints they are subject to: whether a body part can perform a given task well could depend on where it is (e.g., position along an axis). Such constraint would bias the movement of the adaptive peak and might explain some observed patterns of evolution: for example, bipedal tetrapods typically support their weight using their hindlimbs rather than forelimbs (*63*), and arthropod appendages specialized for assisting feeding need to posited near the anterior end (*64–66*).

In addition to the scenarios examined in this study, there are other ways by which novel characters arise from serial homologs. A type of evolutionary change of interest is change in the number of serial homologs; specifically, duplication of body parts could potentiate the evolution of novel character identities under selection for novel functions or division of labor. Mechanisms mediating developmental and selective constraints on the number of serial homologs, however, are poorly understood and likely vary among different types of characters, making it difficult to model the evolution of the number of serial homologs. In particular, it is challenging to distinguish

constraints resulting from selection on the number *per se* and indirect selective constraint mediated by pleiotropic effects of mutations that alter the number of them (e.g., mutations responsible for Pallister–Hall syndrome cause polydactyly along with other symptoms (*67*)). Pleiotropy is known to constrain the evolution of traits that are not themselves under selection, resulting in reduced level of within-population phenotypic variation and evolutionary rate (*68–71*); for discrete traits showing little variation among species, however, it can be even more challenging to tease apart from direct and indirect effects of selection. A type of character that may potentially offer implications for this problem are serial homologs whose number is conserved within some clades but variable in other clades and between clades. For example, the number of cervical vertebrae is highly conserved among mammals (typically seven, with few exceptions) but much more variable in sauropsids, likely due to different levels constraint resulting from pleiotropy (*72–76*). It would be of interest for future studies to compare developmental processes as well as selective constraints in different clades to provide insights into mechanisms underlying constraints on the number of serial homologs.

Another type of genetic change that could lead to novelties is gene or genome duplication. Specifically, duplication of IDGs that are ancestrally shared among serial homologs makes it possible for different duplicates to undergo subfunctionalization and become expressed locally in specific serial homologues, resulting in distinct character identities and potentiating further character state divergence (*36*). Indeed, paralogous genes are known to be involved in specification of identities—e.g., the *Hox* genes specify identities of body parts along the anterior-posterior axis (*13, 77–79*). It is hypothesized that genome duplication facilitated the evolutionary innovations and ultimately diversification in certain clades, such as in teleost fishes (*80, 81*). Genome duplication in the common ancestor of teleosts made it possible for a novel axial patterning pathway to be established (*82–84*), but whether it is responsible for a broader range of novelties as well as species diversity has not been rigorously tested. Gene and genome duplications can be readily modeled in our framework as duplications of entries of **L**, **A**, and/or **B**, and one can examine and compare dynamics of phenotypic evolution in genotypes containing different numbers of gene copies.

In our simulations, structure of the gene regulatory networks underlying development did not change over time. It is plausible, however, that second-order selection could act to optimize their structures, enhancing robustness and/or evolvability. Specifically, it has been hypothesized that such selection has been responsible for modularity of gene regulatory networks controlling

development (*85–88*). In order for second-order selection to work, there must be mutations that modify the distribution of other mutations' effects on gene expression (specifically, correlation between regulatory mutations' effects on gene expression in different serial homologs). The rate and distribution of effects of such modifier mutations, however, are poorly understood, posing a major challenge to modeling and detecting second-order selection. Nevertheless, it is of great interest for future theoretical studies to explore factors that affect efficacy of second-order selection given these settings, starting with arbitrarily defined rates and effect distributions of modifier mutations. Recent years have also seen progress made in predicting regulatory potential of putative *cis*-elements and detecting selection on regulatory activities (*89–95*); findings in this area may shed light on how gene regulatory networks underlying development could potentially be rewired during evolution and help better parameterize models for developmental evolution.

It is worth noting that, it remains unclear whether certain characters are homologous or serially homologous, and different interpretations regarding homology could have different evolutionary implications. An example is the lower jaw of gnathostomes (jawed vertebrates): it is hypothesized that the lower jaw evolved from gill arches, yet there has been mixed evidence and continued debate over this hypothesis (*96–99*). Complicating the problem of homology is the phenomenon known as deep homology—that the same gene(s) or pathways are recruited independently to regulate the development of different characters (*100*). For example, digits of tetrapods and fin rays of ray-finned fishes have shared developmental regulators (*101*), despite digit identities of crown tetrapods originated well after tetrapods split from the rest of Osteichthyes (*102, 103*). For such characters, which did not have a shared ancestral developmental programs to start with, it is no longer reasonable to assume that they have similar ancestral character states, as we did in our simulations. Importantly, notions of character state 'divergence' and 'novelty' would no longer be sensible in the absence of historical continuity. Hence, characterization of homology is highly relevant to parameterization and interpretation of model predictions. Nevertheless, the coevolution deeply homologous characters may still be subject to constraints imposed by their shared developmental regulators; modeling their coevolution would be of great interest for future studies.

The model presented in this study has key implications for phylogenetic comparative analyses aimed at inferring drivers of phenotypic divergence. Recent work has shown that, by integrating information about developmental mechanisms into commonly used phylogenetic models, evolu-

tionary rate estimates are less variable among clades (*43*), indicating developmental constraints can potential lead to spurious macroevolutionary patterns. It is plausible that a broader range of characters are subject to similar problems, and development-informed phylogenetic models will be necessary to disentangle the effect of developmental constraints and other processes of interest. Our modeling framework also has implication for phylogenetic analysis of discrete traits as well as inference of phylogeny based on such traits. Analysis of discrete phenotypic variation usually do not distinguish character identity and state variations and apply the same models of evolution (e.g., (*104–106*)). However, identity and state changes have different genetic mechanisms and are favored by selection under different conditions, and failure to distinguish them may confound inference of evolutionary mechanisms or phylogenetic history (*107*). Hence, it is essential for future studies to consider developmental aspects of characters and give different treatment to different phenotypic changes accordingly.

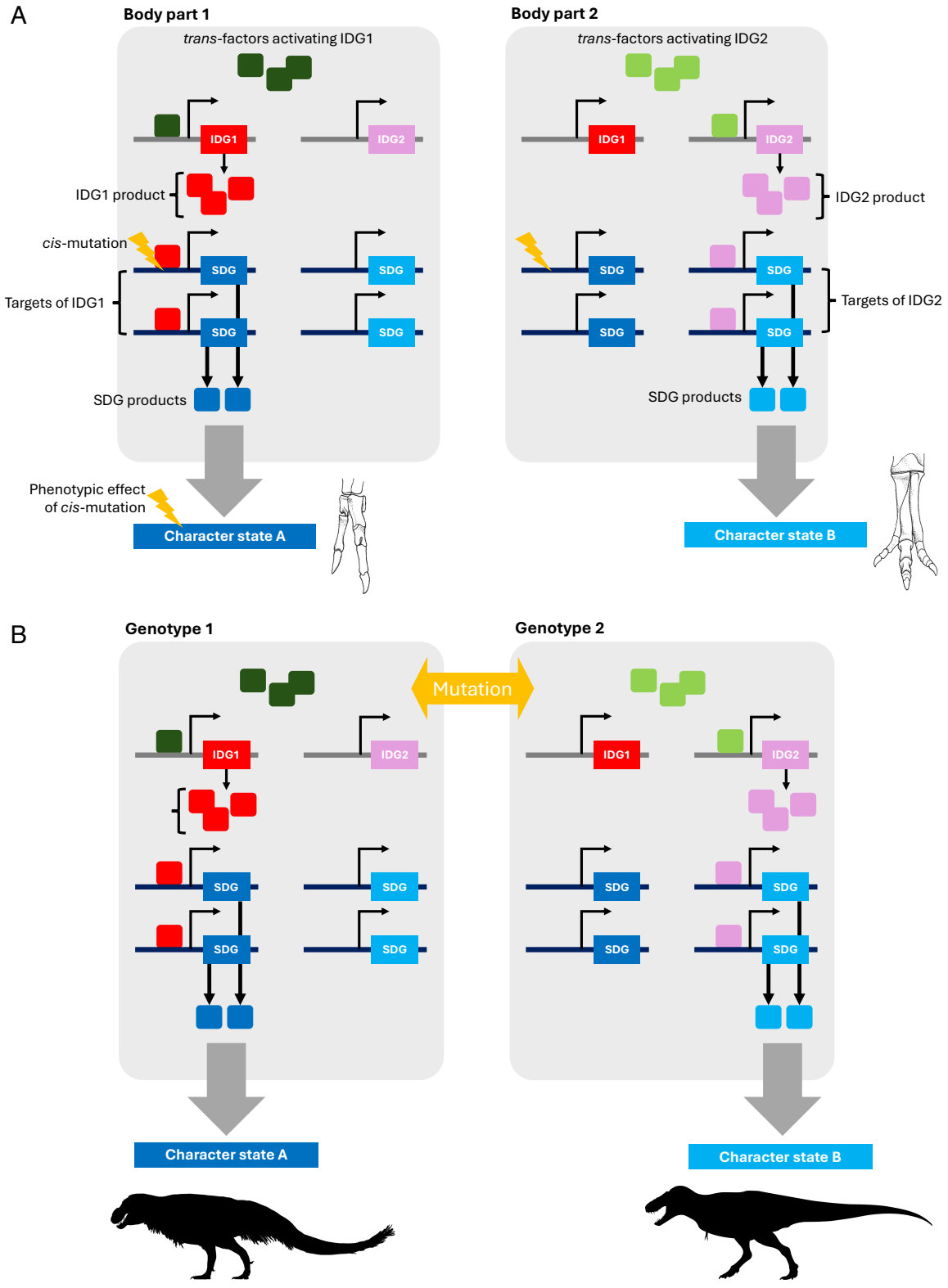
A
Body part 1
trans-factors activating IDG1
IDG1
IDG2
IDG1 product
cis-mutation
SDG
Targets of IDG1
SDG products
Phenotypic effect
of cis-mutation
Character state A
Body part 2
trans-factors activating IDG2
IDG2 product
Targets of IDG2
Character state B
B
Genotype 1
Genotype 2
Mutation
Character state A
Character state B

Figure 1: A schematic illustration for the developmental model presented in this study and two types of evolutionary novelty examined. For a given body part, the local *trans*-regulatory environment determines the expression of the IDGs and thereby determines the expression of SDGs regulated by the IDGs. Expression of the SDGs determines the character state. (A) Two serially homologous body parts with distinct and conserved identities (e.g., hand and foot). The two serial homologs have conserved IDG expression profiles, and mutations can happen in *cis*-elements of SDGs and alter SDGs' response to IDGs, thereby altering character state (e.g., morphology of hand and foot). A mutation in a specific SDG's *cis*-element is shown; as the affected SDG is an exclusive target of one IDG, character state of only one serial homolog is affected. (B) A body part (e.g., skin of a specific body region) whose identity can be altered by mutations that turn on and off master regulator genes (IDGs). Left and right sides correspond to genotypes that can mutate toward each other. The two genotypes have different *trans*-regulatory environments that result in different IDG expression programs, thereby the expression of different SDGs and production of different character states (e.g., feathered and non-feathered states). Two unique targets of each IDG is shown in each panel, whereas common targets of the IDGs are omitted. Images of *Tyrannosaurus rex* hand and foot skeletons in (A) are modified from (*50*). *T. rex* silhouettes in (B) are from PhyloPic (https://www.phylopic.org/), and are created by Matt Martyniuk (left) and Matt Dempsey (right), respectively.

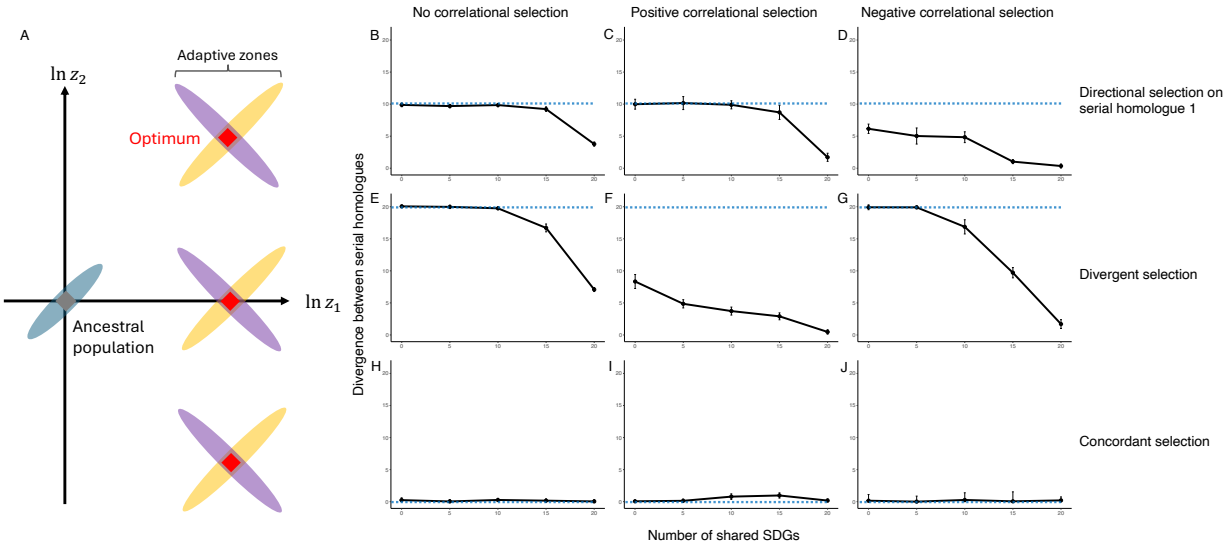

Figure 2: (A) Scenarios of directional selection on serially homologous characters with conserved identities, superimposed onto the same graph. Axes represent character states of two serial homologs ($\ln z_1$ and $\ln z_2$). The origin point is the ancestral state. Ellipse covering the origin point represents an expected distribution of character states produced by mutations when IDGs underlying two serial homologs have shared targets. Red dots represent optimal phenotypes (adaptive peaks). Yellow and purple ellipses represent adaptive zones when positive (yellow) and negative (purple) correlational selection is present, respectively, with their major axes corresponding to the optimal scaling between $\ln z_1$ and $\ln z_2$. (B-J) Character state divergence between two serial homologs at the end of the simulation, calculated as $|\mathrm{E}(\ln z_1) - \mathrm{E}(\ln z_2)|$, where $\mathrm{E}(\ln z_1)$ and $\mathrm{E}(\ln z_2)$ are cross-population means of two serial homologs' log-transformed phenotypic values ($\ln z_1$ and $\ln z_2$) (see Methods). Blue dashed lines correspond to expected levels of divergence when both serial homologs are optimized. Height of each error bar is equal to twice the sum of standard errors of $\mathrm{E}(\ln z_1)$ and $\mathrm{E}(\ln z_2)$ (sample size $n = 10$); lower bound set as zero if below zero. (B-D) Only one serial homolog's character state ($\ln z_1$) is under directional selection. (E-G) Two serial homologs are under divergent selection for different optima. (H-J) Two serial homologs are under concordant selection. Columns corresponds to regimes of correlational selection: no correlational selection (B, E, H), positive correlational selection (C, F, I), and negative correlational selection (D, G, J).

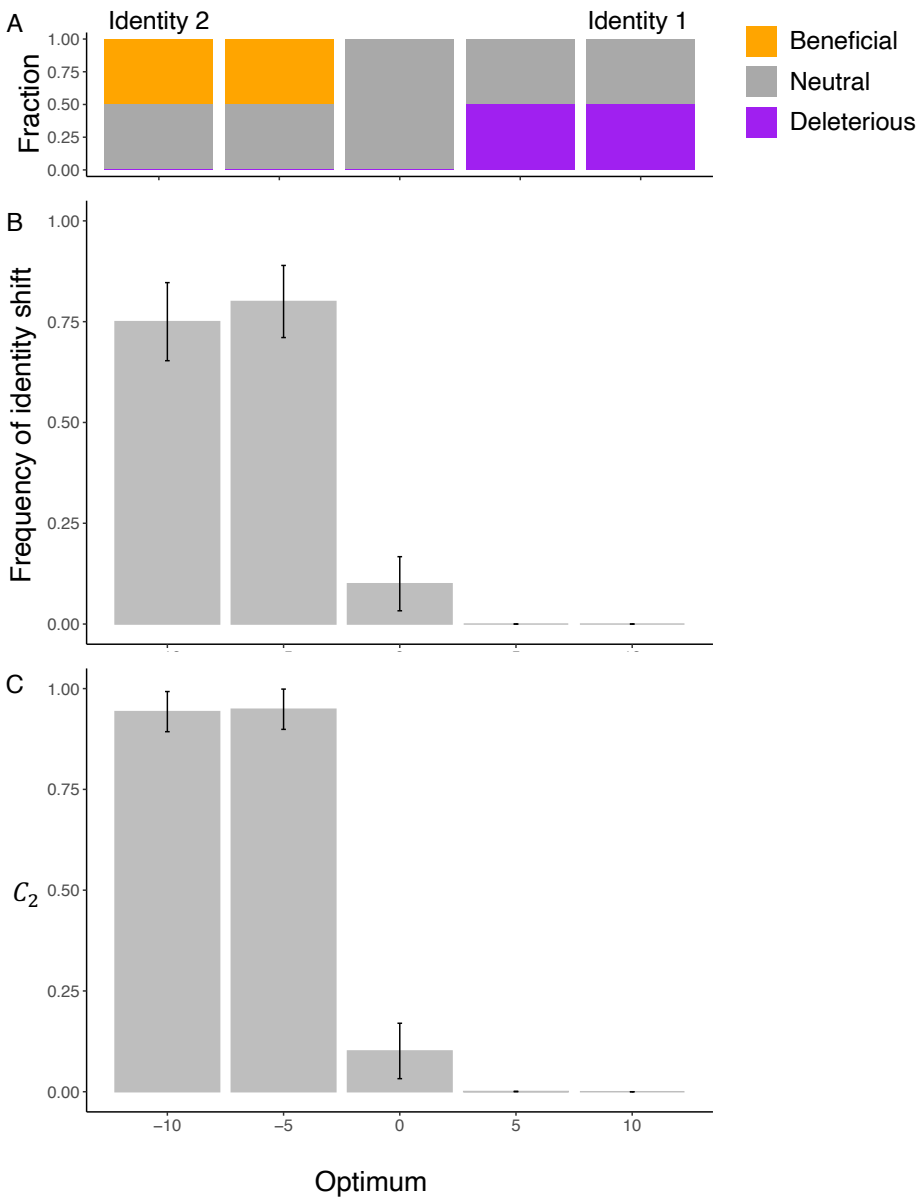

Figure 3: (A) Fitness effects of of mutations that affect the concentration of the morphogen underlying character identity. Colors correspond to three categories of mutations (beneficial, neutral, and deleterious, defined by fitness effect on an ancestral genetic background), with bar heights corresponding to the fraction of mutations that fall into each category. (B) Fraction of simulated populations where the non-ancestral identity I_2 is fixed. (C) Mean *trans*-genotypic value for the expression of the IDG underlying I_2 across populations, as captured by the mean value of the second the element of **C** (C_2). Height of each error bar in (B) and (C) is twice the standard error (sample size $n = 20$).

References and Notes

1. V. L. Roth, On homology. *Biological Journal of the Linnean Society* **22** (1), 13–29 (1984).

2. N. Shubin, C. Tabin, S. Carroll, Fossils, genes and the evolution of animal limbs. *Nature* **388** (6643), 639–648 (1997).

3. G. P. Wagner, *Homology, genes, and evolutionary innovation* (princeton university press) (2014).

4. S. J. Gould, R. C. Lewontin, The spandrels of san marco and the panglossian paradigm: a critique of the adaptationist programme. *Conceptual Issues in Evolutionary Biology* **205**, 79 (1979).

5. J. M. Smith, *et al.*, Developmental constraints and evolution: a perspective from the Mountain Lake conference on development and evolution. *The Quarterly Review of Biology* **60** (3), 265–287 (1985).

6. L. Y. Yampolsky, A. Stoltzfus, Bias in the introduction of variation as an orienting factor in evolution. *Evolution & development* **3** (2), 73–83 (2001).

7. J. L. Hendrikse, T. E. Parsons, B. Hallgrímsson, Evolvability as the proper focus of evolutionary developmental biology. *Evolution & development* **9** (4), 393–401 (2007).

8. K. D. Kavanagh, *et al.*, Developmental bias in the evolution of phalanges. *Proceedings of the National Academy of Sciences* **110** (45), 18190–18195 (2013).

9. J. A. Fritz, *et al.*, Shared developmental programme strongly constrains beak shape diversity in songbirds. *Nature Communications* **5** (1), 3700 (2014).

10. A. Stoltzfus, *Mutation, randomness, and evolution* (Oxford University Press) (2021).

11. P. T. Rohner, D. Berger, Developmental bias predicts 60 million years of wing shape evolution. *Proceedings of the National Academy of Sciences* **120** (19), e2211210120 (2023).

12. P. T. Rohner, D. Berger, Macroevolution along developmental lines of least resistance in fly wings. *Nature Ecology & Evolution* pp. 1–13 (2025).

13. S. B. Carroll, Homeotic genes and the evolution of arthropods and chordates. *Nature* **376** (6540), 479–485 (1995).

14. G. P. Wagner, P. F. Stadler, Quasi-independence, homology and the unity of type: A topological theory of characters. *Journal of Theoretical Biology* **220** (4), 505–527 (2003).

15. G. P. Wagner, The developmental genetics of homology. *Nature Reviews Genetics* **8** (6), 473–479 (2007).

16. J. M. Musser, G. P. Wagner, Character trees from transcriptome data: origin and individuation of morphological characters and the so-called "species signal". *Journal of Experimental Zoology Part B: Molecular and Developmental Evolution* **324** (7), 588–604 (2015).

17. R. W. Warren, L. Nagy, J. Selegue, J. Gates, S. Carroll, Evolution of homeotic gene regulation and function in flies and butterflies. *Nature* **372** (6505), 458–461 (1994).

18. S. D. Weatherbee, G. Halder, J. Kim, A. Hudson, S. Carroll, Ultrabithorax regulates genes at several levels of the wing-patterning hierarchy to shape the development of the Drosophila haltere. *Genes & development* **12** (10), 1474–1482 (1998).

19. S. D. Weatherbee, *et al.*, Ultrabithorax function in butterfly wings and the evolution of insect wing patterns. *Current Biology* **9** (3), 109–115 (1999).

20. J. Deutsch, Hox and wings. *Bioessays* **27** (7), 673–675 (2005).

21. Y. Tomoyasu, S. R. Wheeler, R. E. Denell, Ultrabithorax is required for membranous wing identity in the beetle Tribolium castaneum. *Nature* **433** (7026), 643–647 (2005).

22. B. M. Hersh, *et al.*, The UBX-regulated network in the haltere imaginal disc of D. melanogaster. *Developmental biology* **302** (2), 717–727 (2007).

23. Y. Tomoyasu, Y. Arakane, K. J. Kramer, R. E. Denell, Repeated co-options of exoskeleton formation during wing-to-elytron evolution in beetles. *Current Biology* **19** (24), 2057–2065 (2009).

24. X. Tong, S. Hrycaj, O. Podlaha, A. Popadic, A. Monteiro, Over-expression of Ultrabithorax alters embryonic body plan and wing patterns in the butterfly Bicyclus anynana. *Developmental biology* **394** (2), 357–366 (2014).

25. H. Ohuchi, *et al.*, Correlation of wing-leg identity in ectopic FGF-induced chimeric limbs with the differential expression of chick Tbx5 and Tbx4. *Development* **125** (1), 51–60 (1998).

26. P. Agarwal, *et al.*, Tbx5 is essential for forelimb bud initiation following patterning of the limb field in the mouse embryo. *Development* **130** (3), 623–633 (2003).

27. L. Naiche, V. E. Papaioannou, Loss of Tbx4 blocks hindlimb development and affects vascularization and fusion of the allantois. *Development* **130** (12), 2681–2693 (2003).

28. C. Minguillon, J. Del Buono, M. P. Logan, Tbx5 and Tbx4 are not sufficient to determine limb-specific morphologies but have common roles in initiating limb outgrowth. *Developmental cell* **8** (1), 75–84 (2005).

29. J.-F. Ouimette, M. L. Jolin, A. L'honoré, A. Gifuni, J. Drouin, Divergent transcriptional activities determine limb identity. *Nature communications* **1** (1), 35 (2010).

30. V. Duboc, M. P. Logan, Regulation of limb bud initiation and limb-type morphology. *Developmental Dynamics* **240** (5), 1017–1027 (2011).

31. F. Petit, K. E. Sears, N. Ahituv, Limb development: a paradigm of gene regulation. *Nature Reviews Genetics* **18** (4), 245–258 (2017).

32. R. Shirasaki, S. L. Pfaff, Transcriptional codes and the control of neuronal identity. *Annual review of neuroscience* **25** (1), 251–281 (2002).

33. D. Arendt, The evolution of cell types in animals: emerging principles from molecular studies. *Nature Reviews Genetics* **9** (11), 868–882 (2008).

34. T. Hashimshony, M. Feder, M. Levin, B. K. Hall, I. Yanai, Spatiotemporal transcriptomics reveals the evolutionary history of the endoderm germ layer. *Nature* **519** (7542), 219–222 (2015).

35. K. Kin, M. C. Nnamani, V. J. Lynch, E. Michaelides, G. P. Wagner, Cell-type phylogenetics and the origin of endometrial stromal cells. *Cell reports* **10** (8), 1398–1409 (2015).

36. S. B. Carroll, Evo-devo and an expanding evolutionary synthesis: a genetic theory of morphological evolution. *Cell* **134** (1), 25–36 (2008).

37. R. O. Prum, Development and evolutionary origin of feathers. *Journal of Experimental Zoology* **285** (4), 291–306 (1999).

38. M. A. Norell, X. Xu, Feathered dinosaurs. *Annu. Rev. Earth Planet. Sci.* **33** (1), 277–299 (2005).

39. L. Sallan, Fish 'tails' result from outgrowth and reduction of two separate ancestral tails. *Current Biology* **26** (23), R1224–R1225 (2016).

40. D. M. Raup, Geometric analysis of shell coiling: general problems. *Journal of paleontology* pp. 1178–1190 (1966).

41. D. M. Raup, Theoretical morphology of echinoid growth. *Journal of Paleontology* **42** (S2), 50–63 (1968).

42. I. Salazar-Ciudad, J. Jernvall, A computational model of teeth and the developmental origins of morphological variation. *Nature* **464** (7288), 583–586 (2010).

43. F. A. Machado, *et al.*, Rules of teeth development align microevolution with macroevolution in extant and extinct primates. *Nature Ecology & Evolution* pp. 1–11 (2023).

44. J. DiFrisco, A. C. Love, G. P. Wagner, Character identity mechanisms: a conceptual model for comparative-mechanistic biology. *Biology & Philosophy* **35** (4), 44 (2020).

45. J. DiFrisco, G. P. Wagner, A. C. Love, Reframing research on evolutionary novelty and co-option: character identity mechanisms versus deep homology, in *Seminars in Cell & Developmental Biology* (Elsevier), vol. 145 (2023), pp. 3–12.

46. D. Arendt, *et al.*, The origin and evolution of cell types. *Nature Reviews Genetics* **17** (12), 744–757 (2016).

47. M. P. Harris, J. F. Fallon, R. O. Prum, Shh-Bmp2 signaling module and the evolutionary origin and diversification of feathers. *Journal of Experimental Zoology* **294** (2), 160–176 (2002).

48. F. Prin, D. Dhouailly, How and when the regional competence of chick epidermis is established: feathers vs. scutate and reticulate scales, a problem en route to a solution. *The International journal of developmental biology* **48** (2-3), 137–148 (2004).

49. R. L. Cooper, M. C. Milinkovitch, Transient agonism of the sonic hedgehog pathway triggers a permanent transition of skin appendage fate in the chicken embryo. *Science Advances* **9** (20), eadg9619 (2023).

50. M. J. Benton, *Vertebrate palaeontology* (John Wiley & Sons) (2014).

51. B. C. Haller, P. W. Messer, SLiM 4: multispecies eco-evolutionary modeling. *The American Naturalist* **201** (5), E127–E139 (2023).

52. L. Wolpert, Positional information and the spatial pattern of cellular differentiation. *Journal of theoretical biology* **25** (1), 1–47 (1969).

53. N. M. Young, G. P. Wagner, B. Hallgrímsson, Development and the evolvability of human limbs. *Proceedings of the National Academy of Sciences* **107** (8), 3400–3405 (2010).

54. C. J. Cretekos, *et al.*, Regulatory divergence modifies limb length between mammals. *Genes & development* **22** (2), 141–151 (2008).

55. E. Z. Kvon, *et al.*, Progressive loss of function in a limb enhancer during snake evolution. *Cell* **167** (3), 633–642 (2016).

56. J. L. Mah, C. W. Dunn, Cell type evolution reconstruction across species through cell phylogenies of single-cell RNA sequencing data. *Nature Ecology & Evolution* **8** (2), 325–338 (2024).

57. A. Brückner, *et al.*, Evolutionary assembly of cooperating cell types in an animal chemical defense system. *Cell* **184** (25), 6138–6156 (2021).

58. S. A. Kitchen, *et al.*, The genomic and cellular basis of biosynthetic innovation in rove beetles. *Cell* (2024).

59. C. Rueffler, J. Hermisson, G. P. Wagner, Evolution of functional specialization and division of labor. *Proceedings of the National Academy of Sciences* **109** (6), E326–E335 (2012).

60. A. Holstad, *et al.*, Evolvability predicts macroevolution under fluctuating selection. *Science* **384** (6696), 688–693 (2024).

61. S. J. Arnold, *Evolutionary Quantitative Genetics* (Oxford University Press, Oxford, UK) (2023).

62. M. Pennell, D. Jiang, The macroevolutionary adaptive landscape: more than a metaphor? (2024).

63. A. E. Maher, *et al.*, Body size, shape and ecology in tetrapods. *Nature Communications* **13** (1), 4340 (2022).

64. G. Scholtz, G. D. Edgecombe, The evolution of arthropod heads: reconciling morphological, developmental and palaeontological evidence. *Development genes and evolution* **216**, 395–415 (2006).

65. E. L. Jockusch, Developmental and evolutionary perspectives on the origin and diversification of arthropod appendages. *Integrative and comparative biology* **57** (3), 533–545 (2017).

66. J. Ortega-Hernández, R. Janssen, G. E. Budd, Origin and evolution of the panarthropod head–a palaeobiological and developmental perspective. *Arthropod structure & development* **46** (3), 354–379 (2017).

67. S. Kang, J. M. Graham Jr, A. H. Olney, L. G. Biesecker, GLI3 frameshift mutations cause autosomal dominant Pallister-Hall syndrome. *Nature genetics* **15** (3), 266–268 (1997).

68. M. Turelli, Effects of pleiotropy on predictions concerning mutation-selection balance for polygenic traits. *Genetics* **111** (1), 165–195 (1985).

69. X.-S. Zhang, W. G. Hill, Genetic variability under mutation selection balance. *Trends in Ecology & Evolution* **20** (9), 468–470 (2005).

70. K. McGuigan, L. Rowe, M. W. Blows, Pleiotropy, apparent stabilizing selection and uncovering fitness optima. *Trends in Ecology & Evolution* **26** (1), 22–29 (2011).

71. D. Jiang, J. Zhang, Fly wing evolution explained by a neutral model with mutational pleiotropy. *Evolution* **74** (9), 2158–2167 (2020).

72. F. Galis, Why do almost all mammals have seven cervical vertebrae? Developmental constraints, Hox genes, and cancer. *Journal of Experimental Zoology* **285** (1), 19–26 (1999).

73. F. Galis, *et al.*, Extreme selection in humans against homeotic transformations of cervical vertebrae. *Evolution* **60** (12), 2643–2654 (2006).

74. I. Varela-Lasheras, *et al.*, Breaking evolutionary and pleiotropic constraints in mammals: on sloths, manatees and homeotic mutations. *EvoDevo* **2**, 1–27 (2011).

75. C. Böhmer, O. W. Rauhut, G. Wörheide, Correlation between Hox code and vertebral morphology in archosaurs. *Proceedings of the Royal Society B: Biological Sciences* **282** (1810), 20150077 (2015).

76. R. T. Cerbus, I. Hiratani, K. Kawaguchi, Homeotic and nonhomeotic patterns in the tetrapod vertebral formula. *Proceedings of the National Academy of Sciences* **121** (47), e2411421121 (2024).

77. A. C. Burke, C. E. Nelson, B. A. Morgan, C. Tabin, Hox genes and the evolution of vertebrate axial morphology. *Development* **121** (2), 333–346 (1995).

78. D. M. Wellik, M. R. Capecchi, Hox10 and Hox11 genes are required to globally pattern the mammalian skeleton. *Science* **301** (5631), 363–367 (2003).

79. J. Pascual-Anaya, *et al.*, Hagfish and lamprey Hox genes reveal conservation of temporal colinearity in vertebrates. *Nature Ecology & Evolution* **2** (5), 859–866 (2018).

80. S. M. Glasauer, S. C. Neuhauss, Whole-genome duplication in teleost fishes and its evolutionary consequences. *Molecular genetics and genomics* **289**, 1045–1060 (2014).

81. L. C. Sallan, Major issues in the origins of ray-finned fish (A ctinopterygii) biodiversity. *Biological Reviews* **89** (4), 950–971 (2014).

82. B. Peskin, *et al.*, Notochordal signals establish phylogenetic identity of the teleost spine. *Current Biology* **30** (14), 2805–2814 (2020).

83. L. Sallan, Evolution: Spinal innovation enabled by genome duplication. *Current Biology* **30** (17), R1006–R1008 (2020).

84. K. E. Criswell, J. A. Gillis, Resegmentation is an ancestral feature of the gnathostome vertebral skeleton. *Elife* **9**, e51696 (2020).

85. G. P. Wagner, L. Altenberg, Perspective: complex adaptations and the evolution of evolvability. *Evolution* **50** (3), 967–976 (1996).

86. G. P. Wagner, M. Pavlicev, J. M. Cheverud, The road to modularity. *Nature Reviews Genetics* **8** (12), 921–931 (2007).

87. J. Clune, J.-B. Mouret, H. Lipson, The evolutionary origins of modularity. *Proceedings of the Royal Society b: Biological sciences* **280** (1755), 20122863 (2013).

88. A. Goswami, J. B. Smaers, C. Soligo, P. D. Polly, The macroevolutionary consequences of phenotypic integration: from development to deep time. *Philosophical Transactions of the Royal Society B: Biological Sciences* **369** (1649), 20130254 (2014).

89. L. Tang, *et al.*, Predicting unrecognized enhancer-mediated genome topology by an ensemble machine learning model. *Genome research* **30** (12), 1835–1845 (2020).

90. J. Liu, M. Robinson-Rechavi, Robust inference of positive selection on regulatory sequences in the human brain. *Science advances* **6** (48), eabc9863 (2020).

91. E. D. Vaishnav, *et al.*, The evolution, evolvability and engineering of gene regulatory DNA. *Nature* **603** (7901), 455–463 (2022).

92. G. Schweizer, A. Wagner, Both binding strength and evolutionary accessibility affect the population frequency of transcription factor binding sequences in Arabidopsis thaliana. *Genome Biology and Evolution* **13** (12), evab273 (2021).

93. X. Zhang, B. Fang, Y.-F. Huang, Transcription factor binding sites are frequently under accelerated evolution in primates. *Nature communications* **14** (1), 783 (2023).

94. G. D. Smith, W. H. Ching, P. Cornejo-Páramo, E. S. Wong, Decoding enhancer complexity with machine learning and high-throughput discovery. *Genome biology* **24** (1), 116 (2023).

95. D. Jiang, J. Zhang, Ascertainment bias in the genomic test of positive selection on regulatory sequences. *Molecular Biology and Evolution* **41** (1), msad284 (2024).

96. J. A. Gillis, M. S. Modrell, C. V. Baker, Developmental evidence for serial homology of the vertebrate jaw and gill arch skeleton. *Nature communications* **4** (1), 1436 (2013).

97. T. Miyashita, Fishing for jaws in early vertebrate evolution: a new hypothesis of mandibular confinement. *Biological Reviews* **91** (3), 611–657 (2016).

98. C. Hirschberger, V. A. Sleight, K. E. Criswell, S. J. Clark, J. A. Gillis, Conserved and unique transcriptional features of pharyngeal arches in the skate (Leucoraja erinacea) and evolution of the jaw. *Molecular Biology and Evolution* **38** (10), 4187–4204 (2021).

99. Q. Tian, F. Zhao, H. Zeng, M. Zhu, B. Jiang, Ultrastructure reveals ancestral vertebrate pharyngeal skeleton in yunnanozoans. *Science* **377** (6602), 218–222 (2022).

100. N. Shubin, C. Tabin, S. Carroll, Deep homology and the origins of evolutionary novelty. *Nature* **457** (7231), 818–823 (2009).

101. T. Nakamura, A. R. Gehrke, J. Lemberg, J. Szymaszek, N. H. Shubin, Digits and fin rays share common developmental histories. *Nature* **537** (7619), 225–228 (2016).

102. M. Coates, J. A. Clack, Polydactyly in the earliest known tetrapod limbs. *Nature* **347** (6288), 66–69 (1990).

103. M. I. Coates, The origin of vertebrate limbs. *Development* **1994** (Supplement), 169–180 (1994).

104. M. Pagel, Detecting correlated evolution on phylogenies: a general method for the comparative analysis of discrete characters. *Proceedings of the Royal Society of London. Series B: Biological Sciences* **255** (1342), 37–45 (1994).

105. P. O. Lewis, A likelihood approach to estimating phylogeny from discrete morphological character data. *Systematic biology* **50** (6), 913–925 (2001).

106. A. M. Wright, D. M. Hillis, Bayesian analysis using a simple likelihood model outperforms parsimony for estimation of phylogeny from discrete morphological data. *PLoS One* **9** (10), e109210 (2014).

107. W. P. Maddison, Missing data versus missing characters in phylogenetic analysis. *Systematic Biology* **42** (4), 576–581 (1993).

Acknowledgments

We thank Joanna Wolfe and Mark Kim for helpful comments.

Funding: DJ and LS are supported by Okinawa Institute of Science and Technology Graduate University.

Author contributions: DJ, MP, and LS conceived the project. DJ designed and performed the study. DJ and LS wrote the paper with input from MP.

Competing interests: There are no competing interests to declare.

Data and materials availability: Code and data files are available at `https://github.com/RexJiangEvoBio/novelty_evo_model`.

Supplementary materials

Materials and Methods

Figs. S1 to S6

Table S1

References *(7-107)*

Supplementary Materials for

A general evolutionary model for the emergence of novel characters from serial homologs

Daohan Jiang, Matt Pennell, Lauren. Sallan*

*Corresponding author. Email: lauren.sallan@oist.jp

This PDF file includes:

Materials and Methods

Figures S1 to S6

Table S1

Materials and Methods

Developmental control of character state

Let there be n identity-determination genes (IDGs) and m state-determination genes (SDGs). For a given IDG, the rate at which its gene product's abundance, X_i changes over time is

$$\frac{dX_i}{dt} = C_i L_i - \gamma X_i. \tag{S1}$$

Here, $C_i \geq 0$ is the local *trans*-regulatory environment's effect on the IDG's expression whereas $L_i \geq 0$ is a genotypic value that captures the *cis*-regulatory sequences' effect on the IDG's expression. The gene product's per-molecule decay rate is γ, which is assumed to be equal for all genes under consideration. The equilibrium X_i, which is reached when $\frac{dX_i}{dt} = 0$, is then

$$X_i = \frac{C_i L_i}{\gamma}. \tag{S2}$$

In this study, γ was assumed to be invariable. For convenience, we set its value to be 1. The above equation thus becomes

$$X_i = C_i L_i. \tag{S3}$$

Together, the IDGs' expression levels in a given serial homolog is given by

$$\mathbf{X} = \mathbf{C} \circ \mathbf{L} = \begin{bmatrix} C_1 L_1 \\ \dots \\ C_n L_n \end{bmatrix}, \tag{S4}$$

where $\mathbf{X}$, $\mathbf{C}$, and $\mathbf{L}$ are vectors of length n.

For a given SDG, the rate of change of its gene product abundance Y_i is given by

$$\frac{dY_i}{dt} = \prod_{j=1}^{n} \exp\left(A_{i,j} X_j\right) - \gamma Y_i = \exp\left(\sum_{j=1}^{n} A_{i,j} X_j\right) - \gamma Y_i, \tag{S5}$$

where $\exp\left(A_{i,j} X_j\right)$ represents the overall regulatory effect of the j-th IDG on the i-th SDG while $A_{i,j}$ characterizes regulatory effect per unit expression of the j-th IDG. When $A_{i,j} > 0$, $\exp\left(A_{i,j} X_j\right)$ increase with the expression level of the j-th IDG, X_j, and the regulatory effect is activation; in contrast, when $A_{i,j} < 0$, $\exp\left(A_{i,j} X_j\right)$ declines with X_j, and the regulatory effect is repression. When $\exp\left(A_{i,j} X_j\right) = 1$, which is reached when $X_j = 0$ or $A_{i,j} = 0$, the j-th IDG has no regulatory

effect on the i-th SDG's expression. Interaction between IDGs and SDGs is modeled in such a way that each activator of an SDG is sufficient but not necessary for the SDG's expression. The equilibrium of Y_i, which is reached when $\frac{dY_i}{dt} = 0$, is

$$Y_i = \frac{\exp\left(\sum_{j=1}^{n} A_{i,j} X_j\right)}{\gamma}. \tag{S6}$$

When $\gamma = 1$, the above equation becomes simply

$$Y_i = \exp\left(\sum_{j=1}^{n} A_{i,j} X_j\right). \tag{S7}$$

Together, the SDGs' expression can be written as

$$\mathbf{Y} = \exp(\mathbf{AX}) = \exp\left(\begin{bmatrix} A_{1,1} & \dots & A_{1,n} \\ \dots & \dots & \dots \\ A_{m,1} & \dots & A_{m,n} \end{bmatrix} \begin{bmatrix} X_1 \\ \dots \\ X_n \end{bmatrix}\right) = \exp\left(\begin{bmatrix} \sum_{i=1}^{n} A_{1,i} X_1 \\ \dots \\ \sum_{i=1}^{n} A_{n,i} X_i \end{bmatrix}\right). \tag{S8}$$

Here, $\mathbf{A}$ is an $m \times n$ matrix that summarizes the strength and direction of each IDG's effect on each SDG.

For a given phenotypic trait (z_i), its value is given by

$$z_i = \prod_{j=1}^{m} Y_j^{B_{i,j}}, \tag{S9}$$

which, after log-transformation, becomes

$$\ln z_i = \sum_{j=1}^{m} B_{i,j} \ln Y_j. \tag{S10}$$

Here, $B_{i,j}$ is a parameter characterizing the i-th SDG's effect on z_i per unit expression; $B_{i,j} = 0$ means Y_j has no effect on z_i. Under such a model, when mutations' effects on Y_i are multiplicative, their effects on z_i will be multiplicative as well, and their effects on $\ln z_i$ will be additive.

If the phenotype of interest d-dimensional, the Eqn. (S9) becomes

$$\mathbf{z} = \exp(\mathbf{B} \ln \mathbf{Y}) = \exp\left(\begin{bmatrix} B_{1,1} & \dots & B_{1,m} \\ \dots & \dots & \dots \\ B_{d,1} & \dots & B_{d,m} \end{bmatrix} \begin{bmatrix} \ln Y_1 \\ \dots \\ \ln Y_n \end{bmatrix}\right). \tag{S11}$$

Here, $\mathbf{z}$ is a vector of length d and $\mathbf{B}$ is a $d \times m$ matrix that summarizes SDGs' per-unit-expression effects on phenotypic traits.

Together, the phenotype can be written as a function of **C**, **L**, **A**, and **B**:

$$\mathbf{z} = \exp\left(\mathbf{BA}(\mathbf{C} \circ \mathbf{L})\right). \tag{S12}$$

The above model can be readily applied to discrete character states by implementing a threshold model where potential character states map to non-overlapping phenotypic sub-spaces of **z**.

Mutational input

In our simulations, we mainly considered *cis*-acting mutations affecting expression of the SDGs. Each of these mutations will affect a specific row of **A**. When a mutation that would affect the i-th row of **A** occurs, we would sample a vector $\Delta = [\delta_1, \ldots, \delta_n]$ from a multivariate normal distribution characterized by a covariance matrix **m**. The vector Δ will be added to the i-th row of **A** element-by-element. If the i-th SDG is ancestrally a shared target of two IDGs (e.g., the j-th and k-th IDGs), the corresponding elements of **A** ($A_{i,j}$ and $A_{i,k}$) will have equal values in the ancestor, and the corresponding off-diagonal elements of **m** ($m_{j,k}$ and $m_{k,j}$) will be positive. In our simulations, we had all diagonal elements of **m** equal to 0.01 and all non-zero off-diagonal elements of **m** equal to 0.009. The **m**-matrices of all SDGs were constant throughout our simulations.

There are additional classes of mutations that were not considered for our simulations but can readily be incorporated under our modeling framework. Below is a description of how they would be coded. The first of these are mutations that take place in *cis*-elements (i.e., promoters and enhancers) of the IDGs and affect elements of **L**. When a mutation that would affect a given entry of **L** (i.e., L_i) occurs, a value δ is sampled from a pre-specified distribution. The second class include *trans*-acting mutations that take place in coding regions of IDGs and SDGs; such a mutation can affect all interactions involving the mutated gene. Specifically, if a *trans*-mutation affects an IDG, all elements in the corresponding column of **A** can be affected; it affects an SDG, the corresponding row of **B** can be affected. Another class includes duplication and loss of IDGs and SDGs. Under our model, an IDG's duplication will result in duplication of the corresponding entries of **L** and **C**, whereas an SDG's duplication will cause the corresponding row of **A** and the corresponding column of **B** to be duplicated. Gene loss, on the other hand, will result in removal of the corresponding element(s) in **L**, **C**, **A**, and/or **B**.

Selection on character state

Selection on character states is characterized by a multivariate Gaussian fitness function, specified by an optimal phenotype, $\mathbf{z_{optimal}}$, and a covariance matrix $\mathbf{\Omega}$. Each diagonal element of $\mathbf{\Omega}$ characterizes strength of selection on a phenotypic dimension, while off-diagonal elements characterize correlational selection. Fitness with respect to a multivariate phenotype $\mathbf{z}$ is given by

$$\omega = \exp\left(-\left(\sqrt{\sum_{i=1}^{n} \frac{P_i^2}{2E_i}}\right)\right). \tag{S13}$$

Here, E_i is the i-th eigenvalue of $\mathbf{\Omega}$ and P_i is the i-th element of $\mathbf{P} = (\ln \mathbf{z} - \ln \mathbf{z_{optimal}})\mathbf{E}$, where $\mathbf{E}$ is the eigenvector matrix of $\mathbf{\Omega}$. If an eigenvalue of $\mathbf{\Omega}$ is zero, the corresponding term in Eqn. (S13) ($\frac{{P_i}^2}{2E_i}$) would be dropped. The biological interpretation of such a situation is the lack of selection on a specific phenotypic dimension, in which case the phenotypic dimension subject to no selection should not be considered when calculating fitness.

SLiM simulations

Population genetic simulations were conducted in SLiM (*51*). For each parameter combination, 10 panmictic diploid populations were simulated. There was no gene flow between populations. Each simulation lasted for 10000 generations. Each row of $\mathbf{A}$ corresponds to a genomic element in SLiM. Each genetic element was modeled with a infinite-sites model and has a corresponding distribution of mutations' effects; each time a mutation occurs, its effect would be sampled from the genetic element's corresponding distribution. The recombination rate was 0.5 in all simulations (free recombination), which interprets as that genomic elements under consideration are sparsely distributed along the chromosome. The *cis*-elements of IDGs were not modeled as mutable genomic elements, which interprets as that IDGs are strongly pleiotropic (i.e., involved in the development of additional characters apart from those being examined) such that mutations affecting their expression are too deleterious to contribute to evolution. In simulations of shifting character identity, there are mutations that alter $\mathbf{C}$; genomic loci where such mutations were coded as one genomic element in our simulation, so the rate of such mutations is equal to the per-element mutation rate (see below).

Both Wright-Fisher (WF) and non-WF populations were simulated. For WF simulations, the population size was 1000, mutation rate per genetic element was 10^{-6} per generation. Variances of

Gaussian fitness functions (i.e., diagonal elements of $\mathbf{\Omega}$) were equal to 1. For non-WF simulations, a density-dependent scenario was considered. Reproduction happens at the beginning of each generation and death happens at the end of each generation. The expected number of offspring produced by each individual each time was 1 and was constant through time; phenotype of an individual affects its death probability. Realized fitness of an individual at the end of the t-th generation (given its phenotype) is $\omega_t = \frac{\omega K}{N_t}$, where $0 < \omega \leq 1$ is its fitness with respect to the phenotype and N_t is the population size at the moment. If $\omega \geq 1$, the individual will survive the generation; otherwise, the probability of death would be $1 - \omega$. In all of our non-WF simulations, K was 2000, the initial population size was equal to K, mutation rate was 10^{-5} per genomic element per generation, and variances of Gaussian fitness functions were 50. Such a combination was chosen such that the ancestral populations are likely to persist at a small size without going extinct before undergoing adaptive evolutionary changes.

Parameterization for characters with conserved identities

We considered two serial homologs with distinct identities. Each identity has an underlying IDG. Specifically, we had $\mathbf{L} = \begin{bmatrix} 1 \\ 1 \end{bmatrix}$, $\mathbf{C_1} = \begin{bmatrix} 1 \\ 0 \end{bmatrix}$, and $\mathbf{C_2} = \begin{bmatrix} 0 \\ 1 \end{bmatrix}$ throughout the simulations, where $\mathbf{C_1}$ and $\mathbf{C_2}$ were $\mathbf{C}$ vectors corresponding to two serial homologs, respectively. All simulations started from an ancestral state with $\mathbf{L} = \begin{bmatrix} 1 \\ 1 \end{bmatrix}$. The number of SDGs regulated by each IDG was the same for two IDGs. In our simulations, each IDG has 20 targets. We considered scenarios where 0, 5, 10, 15, and 20 targets are shared by two IDGs. If a given SDG is ancestrally a target of a given IDG, the corresponding $\mathbf{A}$ element is equal to 1 in the ancestor; otherwise, the element is equal to 0. Character states under concern of the two serial homologs (denoted z_1 and z_2 respectively) are one-dimensional, so $\mathbf{B}$ had one row.

Three scenarios of directional selection were considered for our simulations. In the first scenario, where only z_1 is under directional selection, there are $z_{1.optimal} = \exp(\ln z_{1.a} + 10)$ and $z_{2.optimal} = z_{2.ancestral}$, where $z_{1.ancestral}$ and $z_{2.ancestral}$ are ancestral character states of the two serial homologs, respectively, and $z_{1.optimal}$ and $z_{2.optimal}$ are their respective optima. In the second scenario, where two serial homologs are under divergent selection, there are $z_{1.optimal} = \exp(\ln z_{1.a} + 10)$ and

$z_{2.optimal} = \exp(\ln z_{2.a} - 10)$. In the last scenario, where two scenarios are under concordant selection, there are $z_{1.optimal} = \exp(\ln z_{1.a} + 10)$ and $z_{2.optimal} = \exp(\ln z_{2.a} + 10)$. We also simulated evolution under stabilizing selection (i.e., $z_{1.optimal} = z_{1.ancestral}$ and $z_{2.optimal} = z_{2.ancestral}$). Regarding the pattern of correlational selection, we also considered three scenarios. In the first scenario, there is no correlational selection; off-diagonal elements of the selection matrix $\mathbf{\Omega}$ are thus zero. In the second scenario, there is $\boldsymbol{\rho} = \begin{bmatrix} 1 & 0.9 \\ 0.9 & 1 \end{bmatrix}$, where $\boldsymbol{\rho}$ is the correlation matrix corresponding to the selection matrix $\mathbf{\Omega}$. In the last scenario, there is $\boldsymbol{\rho} = \begin{bmatrix} 1 & -0.9 \\ -0.9 & 1 \end{bmatrix}$. Together, a total of 12 combinations of regimes of directional and correlational selection were examined. At the end of the simulations of directional selection, we examined calculated mean values of $\ln z_1$ and $\ln z_2$ for each population. For each regime of selection, we quantified the overall degree of phenotypic divergence between serial homologs as $|\mathrm{E}(\ln z_1) - \mathrm{E}(\ln z_2)|$, where $\mathrm{E}(\ln z_1)$ and $\mathrm{E}(\ln z_2)$ are cross-population means of $\ln z_1$ and $\ln z_2$, respectively.

Parameterization for character with shifting identity

We focused on a single character and its one-dimensional phenotypic value. Two IDGs can potentially be expressed, producing character identities I_1 and I_2, respectively. Each of the two IDGs has 20 distinct target SDGs ancestrally. The two sets of SDGs affect the phenotype differently: for ancestral targets of one IDG, the corresponding elements of $\mathbf{B}$ are equal to 0.25, while for ancestral targets of the other IDG, the corresponding $\mathbf{B}$ elements are equal to −0.25. In our simulations, the effect of mutations on $\mathbf{C}$ is mediated by a latent trait c, which can be interpreted as corresponding to a morphogen's concentration. The ancestral value of c is zero, which means minimal mutational constraint on identity switching and greater role of selection in determining the chance of switching. Effects of mutations on c were sampled from a normal distribution $\mathcal{N}(0, 0.1)$. When $c \geq 0$, $\mathbf{C} = \begin{bmatrix} 1 \\ 0 \end{bmatrix}$; when $c < 0$, $\mathbf{C} = \begin{bmatrix} 0 \\ 1 \end{bmatrix}$. We assumed mutations' effect on IDG expression to be mediated solely by c but not $\mathbf{L}$ such that alteration of IDG expression by mutations are restricted to the body part under consideration but not other parts. We considered scenarios of selection where the optimal phenotype is $\exp(-10)$, $\exp(-5)$, $\exp(0)$, $\exp(5)$, and $\exp(10)$, respectively. For each

setting, we calculated the fraction of populations where the state $\mathbf{C} = \begin{bmatrix} 0 \\ 1 \end{bmatrix}$ is fixed as well as the mean value of the second element of $\mathbf{C}$ (C_2) among populations.

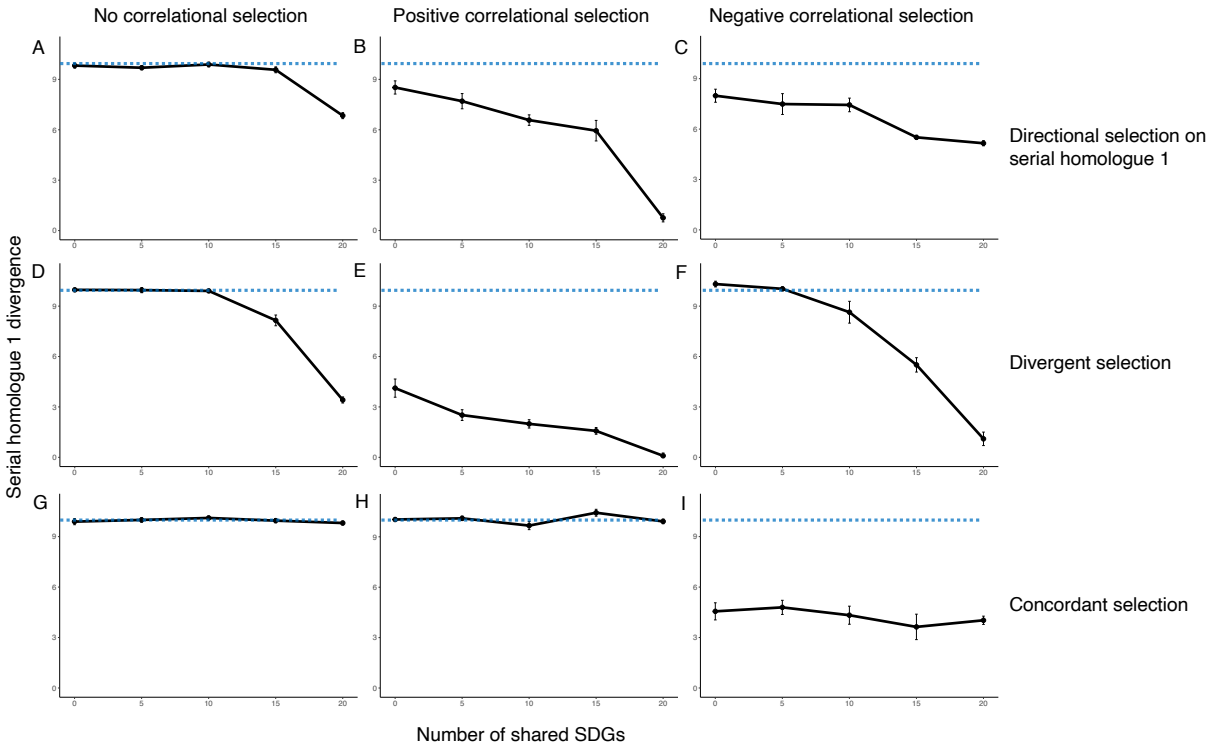

Figure S1: Response of one of two serial homologs with conserved identities to directional selection, quantified as log-fold change in mean phenotype across populations relative to the ancestral state ($\mathrm{E}(\ln z_1) - \ln z_{1.ancestral}$). Scenarios of selection are the same as those in Fig. 2. Blue dashed lines in each panel represent the optimal value for $\ln z_1$, which is the same in all scenarios of selection. Height of each error bar is equal to twice the standard error of $\ln z_1$ (sample size $n = 10$).

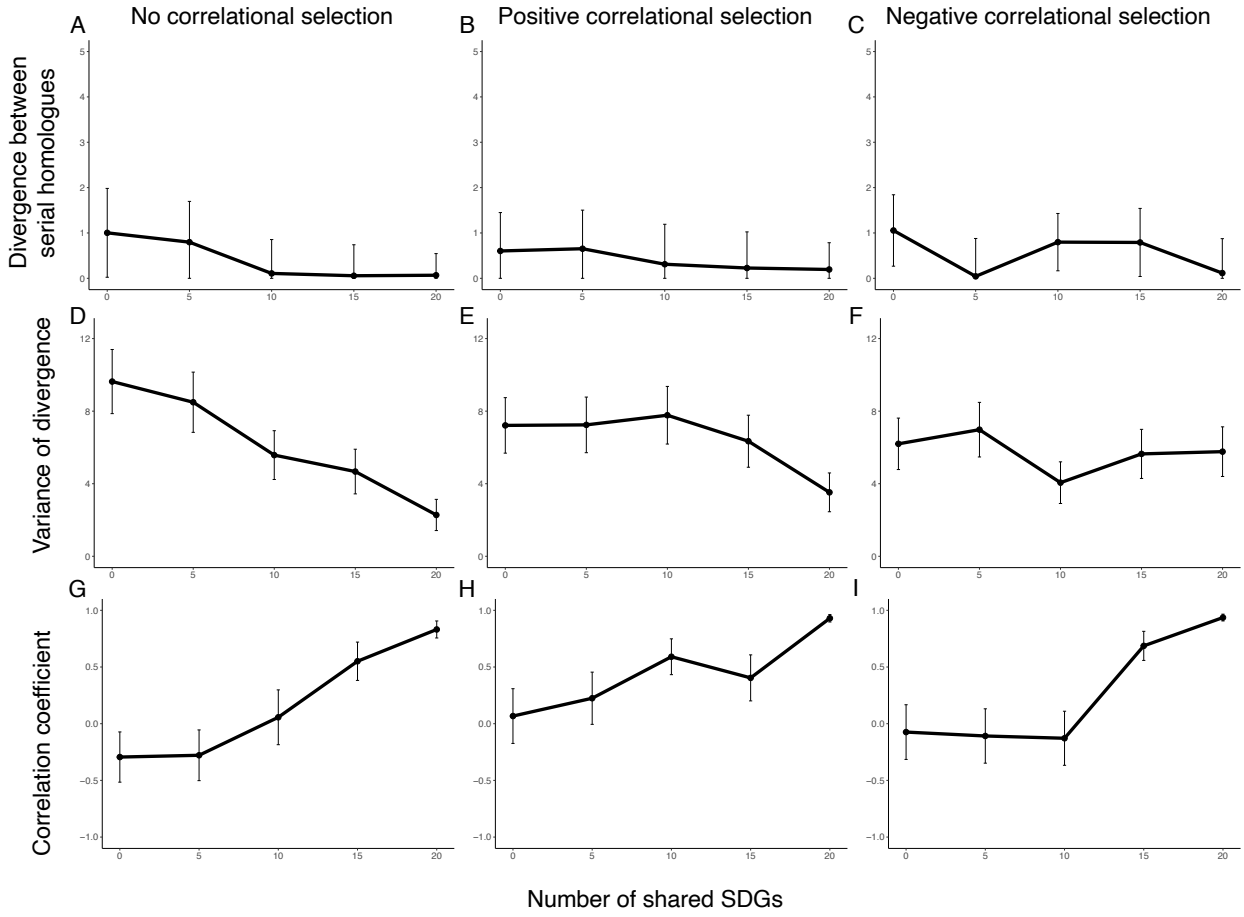

Figure S2: Evolution of serial homologs with conserved identities under stabilizing selection. (A-C) Divergence between character states of two serial homologs. (D-F) Variance of character state divergence across populations, calculated as $\mathrm{Var}(|\ln z_1 - \ln z_2|)$. (G-I) Pearson's correlation coefficient between $\ln z_1$ and $\ln z_2$ across populations.

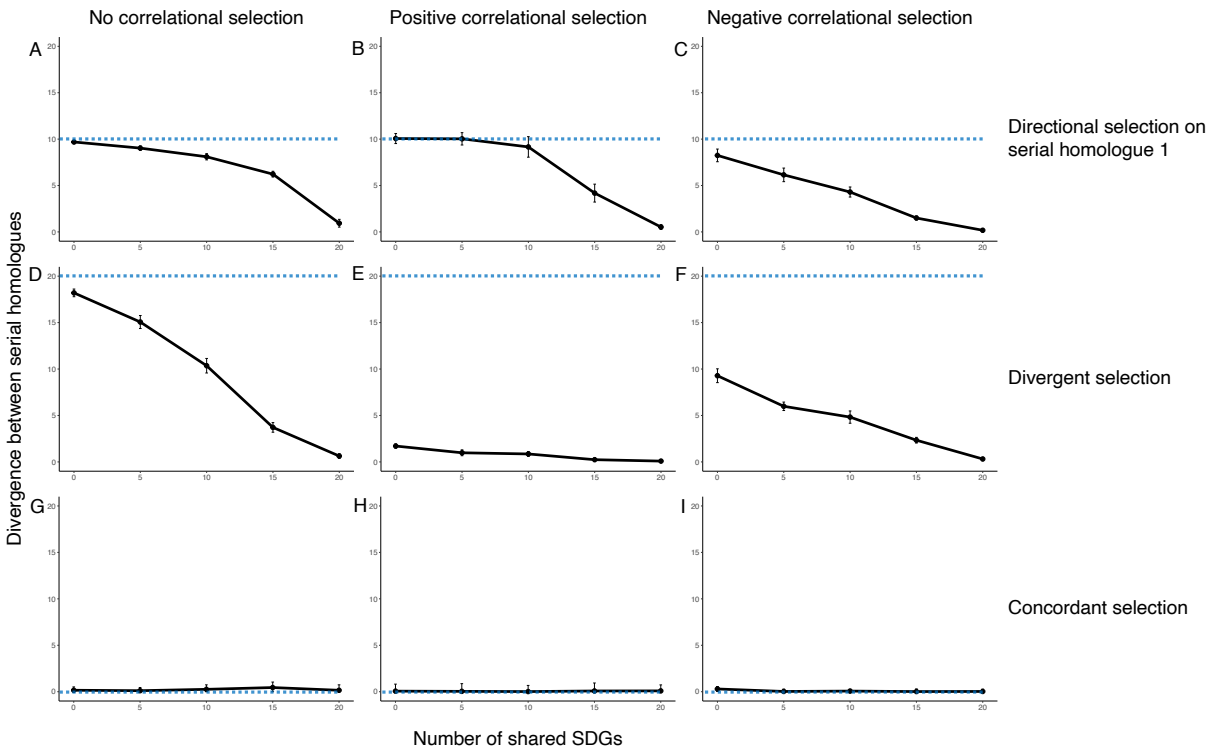

Figure S3: Character state divergence between two serial homologs in non-WF populations. Scenarios of selection are the same as those in Fig. 2. Blue dashed lines correspond to expected levels of divergence when both serial homologs are optimized. Height of each error bar is equal to twice the sum of standard errors of $\mathrm{E}(\ln z_1)$ and $\mathrm{E}(\ln z_2)$ (sample size $n = 10$); lower bound set as zero if below zero.

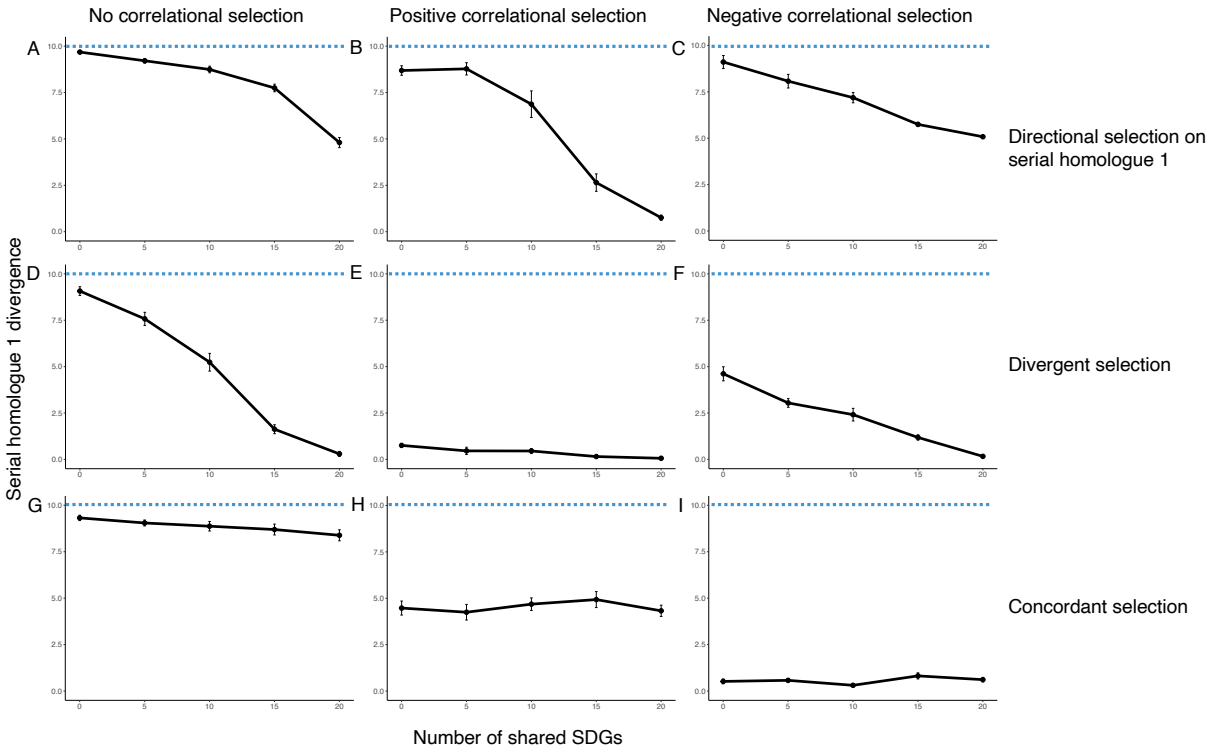

Figure S4: Response of one of two serial homologs with conserved identities to directional selection, quantified as log fold change in mean phenotype across populations relative to the ancestral state ($\mathrm{E}(\ln z_1) - \ln z_{1.ancestral}$), in non-WF populations. Scenarios of selection are the same as those in Fig. 2. Blue dashed lines in each panel represent the optimal value for $\ln z_1$, which is the same in all scenarios of selection. Height of each error bar is equal to twice the standard error of $\ln z_1$ (sample size $n = 10$).

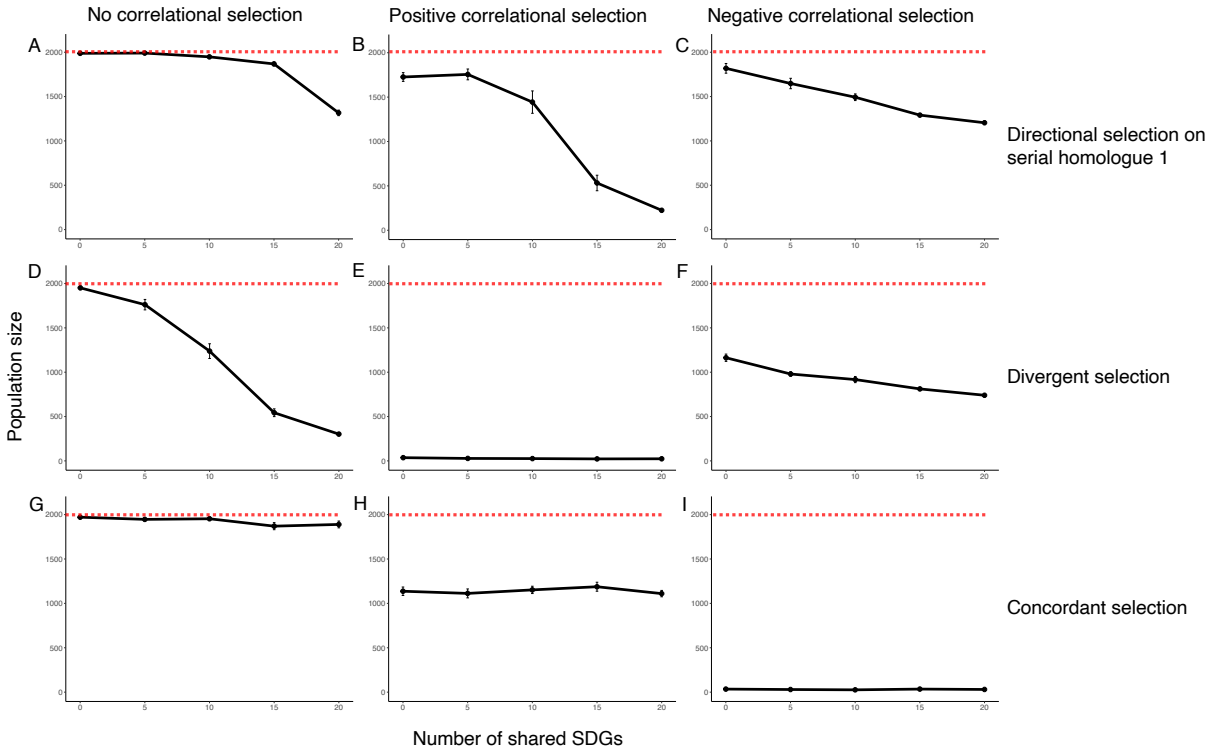

Figure S5: Mean size of non-WF populations at the end of the simulations where serial homolog(s) with conserved identities are under directional selection. Scenarios of selection and notations are the same as those in Fig. 2. Red dashed line represents the carrying capacity, K. Height of each error bars is twice the standard error (sample size n = 10).

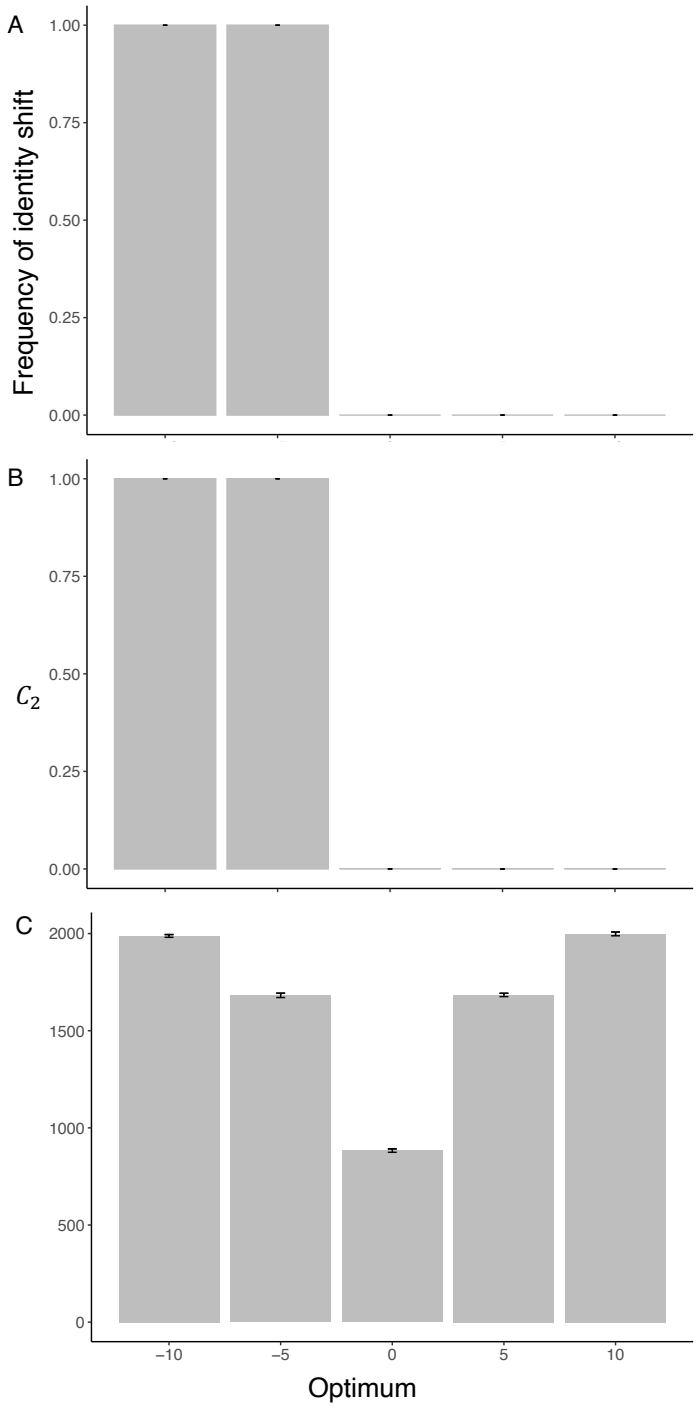

Figure S6: Identity shift in non-WF populations. (A) Fraction of populations where I_2 is fixed. (B) Mean value of the second the element of **C** (C_2) across populations. (C) Mean population sizes at the end of the simulations. Height of each error bars is twice the standard error (sample size $n = 20$).

Table S1: **Definition of parameters.**

Parameter	Definition
$\mathbf{z}$	The multivariate phenotype of a given serial homolog or segment.
$\mathbf{L}$	Vector containing *cis*-genotypic values for expression levels of identity-determination genes (IDGs).
$\mathbf{C}$	Vector containing the local *trans*-regulatory environment's effect on each IDG's expression.
$\mathbf{X}$	Vector containing realized expression levels of IDGs.
$\mathbf{Y}$	Vector containing realized expression levels of state-determination genes (SDGs).
$\mathbf{A}$	Matrix characterizing IDGs' regulatory effects on SDGs.
$\mathbf{B}$	Matrix characterizing SDGs' effect on $\mathbf{z}$.
γ	Decay rate of a gene product.
ω	Fitness of a genotype.
$\mathbf{m}$	Covariance matrix for the effect of *cis*-regulatory mutations on a row of $\mathbf{A}$.
$\mathbf{\Omega}$	Covariance matrix specifying strength of selection and shape of the adaptive landscape. The corresponding correlation matrix is denoted $\boldsymbol{\rho}$.
K	Carrying capacity; the maximum reachable population size when all individuals have the optimal phenotype.